# Influence of ion dose on nanostructure morphology and electrical properties of nitrogen implanted-annealed copper

*Anousheh Kazemeini-Asl*[1], *Majdid M. Larijani*[2], *Vahid Fathollahi*[3]

[1]*Department of Physics, Karaj Branch, Islamic Azad University, Karaj, Iran*
[2]*Nuclear Science and Technology Research Institute (NSTRI), P.O. Box 31485-498, Karaj, Iran*
[3]*Nuclear Science Research School, NSTRI, P.O. Box 14395-836, Tehran, Iran*
*E-mail: mmojtahedzadeh@nrcam.org*

Published in Micro & Nano Letters; Received on 17th June 2014; Revised on 15th September 2014; Accepted on 15th October 2014

Cu thin films sputter-coated on single crystals of silicon were implanted with 30 keV nitrogen ions under various doses from $1.9 \times 10^{17}$ to $5.7 \times 10^{17}$ ions/cm$^2$. The prepared samples were subsequently annealed in nitrogen atmosphere. The grazing incidence X-ray diffraction analysis revealed that in addition to the crystalline copper nitride phase, copper azides were developed by nitrogen ion implantation. With an increase of the implantation dose to $2.3 \times 10^{18}$ ions/cm$^2$, much of the Cu film was transformed to the crystalline $Cu_3N$ phase. Furthermore, the effect of nitrogen ion implantation on Cu thin films under various doses was investigated. The structural properties, morphology and sheet resistance of samples were investigated by grazing incidence X-ray diffraction, atomic force microscopy, field emission scanning electron microscopy and four-point probe techniques, respectively. In addition, the dependence of resistivity of the implanted samples on the implantation dose as well as structural properties is discussed.

**1. Introduction:** During the last two decades, interest in copper nitride ($Cu_3N$) thin films has been motivated by its potential applications as a new material in the recording and electronics industries.

$Cu_3N$ is thermally unstable and decomposes at relatively low temperatures into metallic copper and nitrogen [1–5]. The decomposition can also be induced by irradiation with electrons [5] and laser pulses [6]. This suggests possible applications in write-once optical recording media [7] and electron-induced lithography [5].

$Cu_3N$ crystallises in a cubic anti-$ReO_3$-type structure (with a lattice constant of 0.3815 nm) where the face-centred-cubic close-packed sites are vacant [3]. It is a metastable semiconducting material with a theoretical energy gap of about 0.5 eV [8], whereas experimental values are reported in the range of 0.25–1.9 eV [3, 4, 9–13]. In fact, depending on the chemical composition and stoichiometry of Cu–N compounds, their electrical and optical properties may change remarkably. For instance, although $Cu_4N$ exhibits fully metallic properties [8], $Cu_3N$ behaves as a semiconductor [4, 13]. It is believed that by changing deposition conditions, the stoichiometry of nitride films can be tuned from nitrogen deficient to nitrogen rich [4, 12, 13].

The physical properties of $Cu_3N$ films reported in the literature are dispersed and inconsistent. For instance, the lattice constant of cubic $Cu_3N$ varies from 0.3815 to 0.3885 nm [3, 14, 15], the electrical resistivity spans a large range from $2 \times 10^{-5}$ to $2 \times 10^{3}$ Ω cm [4, 9, 10, 12–15] and the thermal decomposition temperature is estimated to be between 100°C and 470°C [1–5, 7].

The large discrepancy in the reported data originates not only from uncertainty in the analysing methods, but also from the unstable nature of $Cu_3N$. In fact, the weak Cu–N bond is responsible for the instability of $Cu_3N$ [4, 10, 12]. Moreover, $Cu_3N$ samples can undergo immediate changes on irradiation of energetic particle beams during material characterisation. Therefore, the measured values of physical properties depend strongly on the sample condition and the employed analysing techniques [4].

Ion implantation is known as a powerful technique for inducing the development of new phases in thin metal films or in the near-surface region of bulk materials [16–18]. Direct nitrogen implantation into metals can lead to the formation of metal nitrides at room temperature, while employing conventional techniques such as nitriding for the synthesis of most metal nitrides requires high-temperature processing [16].

The aim of the work reported in this Letter was to investigate the effect of direct nitrogen ion implantation in sputtered copper films on silicon. We report the formation of the nitride phase in Cu film and its dependence on the nitrogen ion dose. The structural properties, surface morphology and electrical properties of modified Cu films as a function of the nitrogen ion dose are studied.

**2. Experimental procedure:** Thin films of copper were deposited by the single ion beam sputtering method onto Si (1 0 0) substrates (p-type, 1–3 Ω cm, $0.8 \times 0.6 \times 0.25$ cm$^3$) at 300°C. Prior to deposition, Si substrates were ultrasonically cleaned in acetone and ethanol. During sputtering, pure argon is admitted to the chamber at a flow rate of 20 sccm to maintain a pressure of $1.16 \times 10^{-2}$ Pa inside the chamber. The incident ion current on pure copper target was kept fixed at 20 mA for all the prepared samples.

Two series of samples were prepared. In the first series, the sputtering time was 30 min and the Cu films were 620 nm-thick measured by a stylus profilometer (Dektak III). In this series, one of the samples was retained as the untreated reference and the others were implanted by nitrogen ions produced by a Kaufman ion beam source at various doses ranging from $1.9 \times 10^{17}$ to $5.7 \times 10^{17}$ ions/cm$^2$ as indicated in Table 1.

The energy of the nitrogen ion beam was set at 30 keV during bombardment of the Cu/Si system. The nitrogen current density of 8.7 μA/cm$^2$ was kept constant for all the implanted samples of the first series. Owing to the ion bombardment, the temperature of the Cu films was measured to increase up to 115°C. After the nitrogen ion implantation, samples of the first series were annealed at 200°C in nitrogen atmosphere for 120 min.

For preparation of the second series of samples (samples $M_0$ and $M_1$), sputtering time was reduced to 15 min. Therefore, thinner Cu films (390 nm thick) were deposited on the Si substrates. One of the samples was retained as a reference and the other one (sample $M_1$) was implanted by nitrogen ions at the dose of $2.3 \times 10^{18}$ ions/cm$^2$. The energy of the nitrogen ion beam was again 30 keV and the current density was 175 μA/cm$^2$. Sample $M_1$ of the second series was annealed at 200°C in nitrogen atmosphere for 180 min. The experimental parameters for the preparation of the nitrogen implanted Cu/Si samples are outlined in Table 1.

**Table 1** Experimental parameters for preparation of nitrogen implanted Cu/Si samples, subsequently annealed at 200°C

| Sample code | Dose, ions/cm$^2$ | Nitrogen ion energy, keV | Implantation time, min | Cu/Si temperature during ion implantation, °C | Annealing time, min |
|---|---|---|---|---|---|
| $A_0$ | untreated | untreated | – | – | – |
| $A_1$ | $1.9 \times 10^{17}$ | 30 | 60 | 100 | 120 |
| $A_2$ | $2.8 \times 10^{17}$ | 30 | 90 | 110 | 120 |
| $A_3$ | $3.8 \times 10^{17}$ | 30 | 120 | 110 | 120 |
| $A_4$ | $5.7 \times 10^{17}$ | 30 | 180 | 115 | 120 |
| $M_0$ | untreated | – | – | – | – |
| $M_1$ | $2.3 \times 10^{18}$ | 30 | 180 | 125 | 180 |

The structural and electrical properties of the samples were investigated with different methods. The microstructure of the samples was investigated using the grazing incidence X-ray diffraction (GIXRD) technique. The X-ray diffractometer was a Philips X'pert system using CuK$\alpha$ radiation (wavelength = 1.5405 Å and incidence angle = 1°) with a tungsten filament at 40 kV, 30 mA and step size of 0.02°. The morphology and roughness of the samples modified by ion implantation were studied using atomic force microscopy (AFM) and scanning electron microscopy (SEM), respectively. The employed facilities were AF microscope (SPM Auto Probe CP, Park Scientific Instruments, USA) with a low-stress silicon nitride tip of less than 200 Å radius and a tip opening of 18° and a field emission scanning electron microscope (FE-SEM, Hitachi S4160, Japan). The AFM analysis was carried out at contact mode with a scan size of $5 \times 5$ μm$^2$. The sheet resistance, Ω/□, of the films was measured using a four-point probe technique [Signaton, Keithley 224 programmable current source and 196 digital multimeters (DMMs)].

## 3. Results and discussion

3.1. Crystallography and nanostructure of the films: Figs. 1*a* and *b* show the GIXRD spectra of untreated and implanted–annealed Cu thin films as a function of nitrogen dose in the two series of samples. The spectra are limited to a region from $2\theta = 20°$ to 60°. In the samples of the first series (Fig. 1*a*), the prominent peaks are Cu (1 1 1) and Cu (2 0 0) for all doses. In the untreated sample of the second series (i.e. sample $M_0$), the intensity of the observed Cu peaks is lower than those of sample $A_0$ because of the lower Cu film thickness in sample $M_0$. Furthermore, the peak of CuO is observed in both the implanted and the untreated samples in the first series (Fig. 1*a*) as well as the untreated sample in the second series (Fig. 1*b*). Development of copper oxides in the untreated and implanted samples of both series could be justified by the presence of oxygen as an impurity both in the experimental chamber and in the argon and nitrogen supply cylinders employed for sputtering and ion implantation.

The GIXRD spectra of the implanted samples show that copper azides such as $CuN_3$ with a tetragonal structure and $CuN_6$ with an orthorhombic structure in both series of samples are developed after the post-implantation annealing process. These results indicate that the nitrogen content of post-implanted annealed Cu films in both series have reached the value which is required for the stoichiometric development of the copper azide phase ($CuN_3$). According to the literature, this value is 18% nitrogen in Cu [19]. A small peak of $Cu_3N$ (2 0 0) was also observed at $2\theta = 47.78°$ for all the implanted samples. Nitrogen is reported to be insoluble in copper using conventional techniques [1].

However, it can form metastable compounds with copper by ion implantation [18]. As mentioned in the literature [20], the enthalpy of the formation of $Cu_3N$ is +47.5 kJ/mol. In fact, owing to the high positive values of enthalpy ($\Delta H_f$) reported for copper azide (+253.1 kJ/mol) [21], formation of these phases cannot be predicted by the conventional principles of equilibrium thermodynamics.

As can be seen in the GIXRD spectra of Figs. 1*a* and *b*, direct nitrogen ion implantation could lead to the formation of these phases. The reaction energy for the formation of copper azides is likely provided by ion implantation to overcome the undesired thermodynamic factor [22].

Using the SRIM or TRIM2000 code (http://www.srim.org), the average projected range and straggling of the 30 keV nitrogen ion implanted in Cu thin films was found to be $R_p = 32.4$ nm and $\Delta R_p = 24.1$ nm, respectively. Since the depth of the implanted ions is much lower than the Cu film thickness, only a very thin layer of Cu film is nitrided and the rest of the Cu film remained intact. This is why the Cu peaks could be observed even in the GIXRD pattern of the sample with the highest dose of implantation in the first series (Fig. 1*a*).

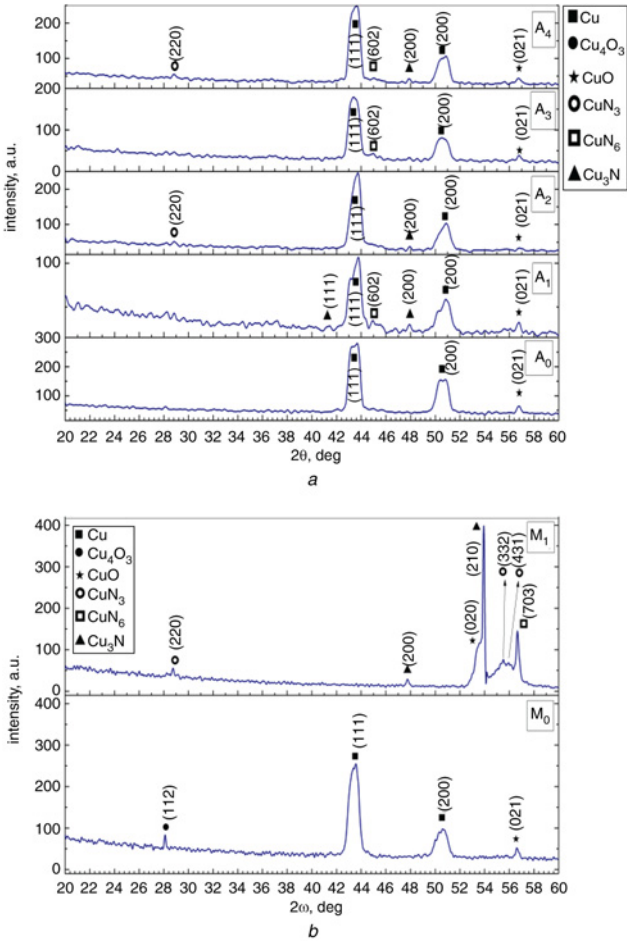


**Figure 1** *XRD patterns*
*a* Sample $A_0$, untreated 620 nm-thick Cu film and samples $A_1$–$A_4$, Cu films implanted with nitrogen ions at different doses of $1.9 \times 10^{17}$ to $5.7 \times 10^{17}$ ions/cm$^2$ and subsequently annealed at 200°C for 120 min
*b* Sample $M_0$, untreated 390 nm-thick Cu film and sample $M_1$, Cu film nitrogen implanted at the dose of $2.3 \times 10^{18}$ ions/cm$^2$, and subsequently annealed at 200°C for 180 min




doi: 10.1049/mnl.2014.0287

Fig. 1*b* shows the XRD spectra of samples $M_0$ (untreated) and $M_1$ (implanted–annealed). It is clear that the Cu film of sample $M_0$ is grown as polycrystalline similar to that of sample $A_0$, although due to its lower thickness, the intensity of the copper peaks is less intense. In the XRD spectrum of sample $M_1$, which is nitrogen implanted with $2.3 \times 10^{18}$ ions/cm$^2$ and post-annealed at 200°C in nitrogen atmosphere for 180 min, several peaks including the preferred orientation of $Cu_3N$ (2 1 0), as well as copper azide peaks of $CuN_6$ (7 0 3), $CuN_3$ (2 2 0), $Cu_3N$ (3 3 2) and $CuN_3$ (4 3 1) are observed. On the other hand, in the XRD spectrum of sample $M_1$, no peak corresponding to Cu is observed. This means that a higher thickness of Cu film in this sample is converted to the $Cu_3N$ phase in comparison with the samples of the first series. This is because the dose and annealing time in the second series are higher than in the first series. In fact, increasing the dose intensifies the formation of the $Cu_3N$ phase. Moreover, the augmentation of annealing time from 120 to 180 min can result in the higher penetration of nitrogen atoms into the Cu film [23], leading to more crystallisation of the $Cu_3N$ amorphous phase because of surface diffusion and bulk diffusion [24]. As mentioned earlier, the thermal instability of $Cu_3N$ film because of irradiation with electrons or laser pulses leads to its decomposition into metallic cupper and nitrogen. This behaviour of $Cu_3N$ could be exploited in a number of applications such as optical recording and electron lithography [5, 7].

The surface morphology of the untreated and post-implanted annealed Cu films in the two series of samples was studied by AFM in a scanning area of $5 \times 5$ μm$^2$.

In Fig. 2, three-dimensional (3D) AFM images of untreated and nitrogen ion implanted Cu/Si (1 0 0) samples are shown. The large grain size and the presence of deep grooves in the 3D images of the untreated Cu/Si sample (sample $A_0$) in Fig. 2*a* reveal that the surface diffusion of sputtered adatoms during sputtering has led to the adhesion of adatoms to previously formed grains rather than filling the grooves. The grain size of films obtained from the 2D AFM images using the Gwyddion code in the first series before implantation is about 200 nm and shows no significant variation after the post-implantation annealing process up to $5.7 \times 10^{17}$ ions/cm$^2$. At $5.7 \times 10^{17}$ ions/cm$^2$, the grain size is reduced to 170 nm. In the samples of second series, a decrease of grain size from 70 to 50 nm is also observed after ion implantation. This reduction in grain size is due to the grain boundary sputtering and etching process which becomes significant at high doses. According to the AFM results, the average roughness of the films in the first series is about 20 nm for samples $A_1$–$A_3$ and then increases to 28 nm at $5.7 \times 10^{17}$ ions/cm$^2$ for sample $A_4$ probably because of the different sputtering rates of the film surface.

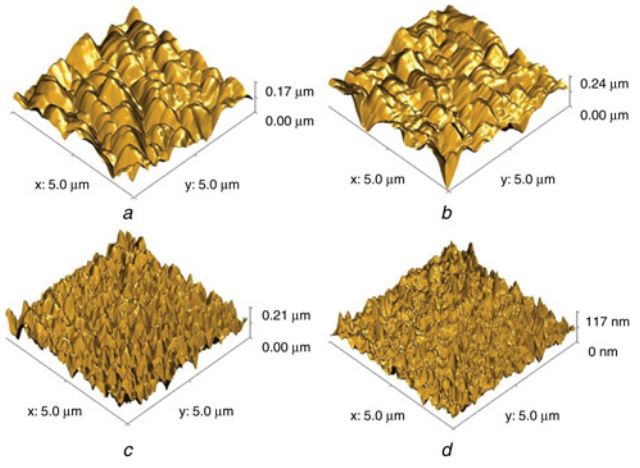


**Figure 2** *3D AFM images of samples*
*a* $A_0$, untreated Cu/Si with 620 nm-thick Cu film
*b* $A_4$, nitrogen implanted Cu/Si with $5.7 \times 10^{17}$ ions/cm$^2$ and annealed at 200°C for 120 min
*c* $M_0$, untreated Cu/Si with 390 nm-thick Cu film
*d* $M_1$, nitrogen implanted Cu/Si with $2.3 \times 10^{18}$ ions/cm$^2$ and annealed at 200°C for 180 min

It seems that the grooves present at the surface of sample $A_0$ have a sputtering rate higher than the grown grains. The grains of sample $M_1$ in comparison with those of sample $M_0$ seem to be less uniform in size and shape (Figs. 2*c* and *d*) because of the formation of new phases after the post-implantation annealing process as revealed by the XRD patterns. In the second series, the average roughness decreases from 22 to 9 nm after implantation. As shown in Fig. 2*d*, the appearance of small grains, which is probably due to the formation of the new phase, results in the reduction of average roughness by filling the grooves and the cavities on the surface of the films. Fig. 3 shows SEM images of the untreated Cu/Si sample with the 390 nm-thick Cu film (sample $M_0$) and the Cu/Si sample implanted at the dose of $2.3 \times 10^{18}$ ions/cm$^2$ (sample $M_1$).

Observation of the grooves on the surface of the untreated sample in Fig. 3*a* indicates that Cu films agglomerate into discrete islands and Cu film grows as the islands layer [25]. Moreover, the presence of nanometre-sized grains in the channels and on the larger grains shows that this sample is in the secondary nucleation process while the film is grown non-uniformly.

As we can see in Fig. 3*b*, the surface morphology of the Cu film is completely changed from a slice-like structure to a uniform structure composed of many crystallites on the surface after the post-implantation annealing process. It seems that the space between the slices is filled by the atoms which are displaced on the surface by the ion energy transfer mechanism and generation of the new phases.

3.2. Electrical properties of the films: The sheet resistance of the untreated and post-implanted annealed Cu films against the nitrogen ion dose for the samples of series 1 is shown in Fig. 4. As can be seen in this Figure, nitrogen ion implantation leads to an increase in the sheet resistance of the copper films. In the samples of series 1, a maximum sheet resistance of 0.11 Ω/□ is measured for the 620 nm-thick copper film which is implanted with the nitrogen ion dose of $5.7 \times 10^{17}$ ions/cm$^2$. It is evident from Fig. 4 that the sheet resistance values have an ascending trend with the increase of the nitrogen ion dose.

The increase in the sheet resistance of metals may be due to several reasons as follows:

(i) By introduction of nitrogen, sheet resistance increases since nitrogen as an impurity leads to an increase in the electron scattering. The electrical resistivity of metals results from the scattering of

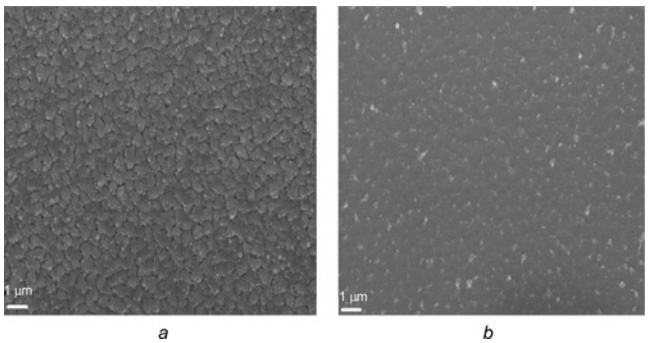


**Figure 3** *FESEM images of Cu/Si (100) samples*
*a* Untreated sample with 390 nm-thick Cu film
*b* Implanted sample with $2.3 \times 10^{18}$ ions/cm$^2$, subsequently annealed at 200°C for 180 min

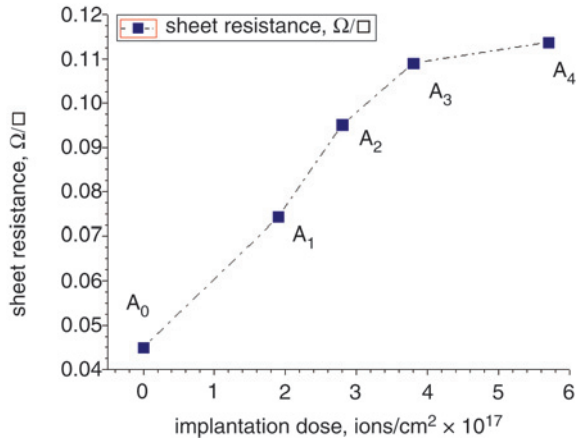


**Figure 4** *Variation of sheet resistance of untreated (sample $A_0$) and post-implanted annealed Cu films (samples $A_1$–$A_4$) against ion implantation dose in the samples of series1*

electrons. The electronic wave can be scattered by interaction with impurity atoms owing to the electrostatic forces.

(ii) Ion implantation leads to the development of crystalline defects and dislocations as well as surface erosion of the films [16]. These defects act as a barrier against movement of carriers. By increasing the implantation dose, surface roughness of the ion implanted copper films increases. This could in turn increase the surface scattering and thus reduce the conductivity and increase the sheet resistance of the films. In our case, the effect of roughness on increase of sheet resistance could be neglected since the variation of roughness at different doses is not significant.

(iii) XRD results confirm that nitrogen ion implantation and subsequent annealing lead to the formation of $Cu_3N$ composition and copper azides. They also show that a higher ion implantation dose intensifies the formation of copper azides and $Cu_3N$ phases. As the $Cu_3N$ phase shows semiconductor behaviour [4, 13], development of $Cu_3N$ results in an increase in the sheet resistance of the implanted copper film. Of course, the presence of various other phases including copper azides – whose lattice structures (tetragonal and orthorhombic) and lattice constants are different from those of Cu and $Cu_3N$ – could also be regarded as a major reason for the increase in sheet resistance of the film [14].

From the data shown in Table 2, it is evident that the sheet resistance of sample $M_1$ in the second series is considerably increased compared to that of untreated copper film and those of post-implanted annealed copper films in the first series (Fig. 4). The abrupt and considerable increase in sheet resistance in Table 2 could be assigned to the disappearance of the Cu phase on the surface and the formation of a preferential semiconducting phase of $Cu_3N$ as well as the formation of compositions such as $CuN_3$ and $CuN_6$.

We notice that sample $A_0$ (620 nm-thick copper film) has a sheet resistance of $4.5 \times 10^{-2}$ Ω/□ and resistivity of $\rho = 2.8$ μΩ cm and sample $M_0$ (390 nm-thick copper film) has a sheet resistance of $6.3 \times 10^{-1}$ Ω/□ and resistivity of $\rho = 24.57$ μΩ cm. Also, the resistivity of sample $A_0$ is still higher than the resistivity of bulk copper (1.67 μΩ cm) [26, 27].

**Table 2** Comparison of sheet resistance (Ω/□) of untreated (sample $M_0$) and implanted-annealed (sample $M_1$) samples in the second series

| Sample code | Sheet resistance, Ω/□ |
|---|---|
| $A_0$ | $4.5 \times 10^{-2}$ |
| $M_0$ | 0.63 |
| $M_1$ | $3.75 \times 10^{+3}$ |

Based on the literature [28, 29], the resistivity of a film depends on electron scattering on the surface, interface and grain boundary. Increase in the resistivity of copper film compared to that of bulk copper may be due to degrees of irregularities and defects such as voids and impurities in the copper film. The presence of CuO and $Cu_4O_3$ phases in the XRD pattern of the prepared films could also be a reason for the higher resistivity of copper film. Anyway, the effect of film density on resistivity could also be discussed [27]. By comparison of the sheet resistance of sample $M_0$ (390 nm-thick copper film) with that of sample $A_0$ (620 nm-thick copper film) in Table 2, one could readily find that the sheet resistance of copper film in the second series of samples is nearly two orders of magnitude higher than that of copper film in the first series of samples.

It is well known that in metallic films grown under similar conditions, thicker films result in lower resistivity of films [26, 29]. This is because of interface electron scattering and grain boundary scattering which could be explained by the FS-MS combined theory [29].

The higher sheet resistance could be assigned to the higher scattering of electrons in the thinner films. It should also be noted that the grains of the copper film in sample $M_0$ are smaller compared to those of sample $A_0$ because of the longer deposition time of sample $A_0$ (30 min) compared to that of sample $M_0$ (15 min) [26]. In fact, in samples with smaller grains, one could expect higher sheet resistance as the electrons are faced with more grain boundaries and are therefore scattered more.

**4. Conclusion:** In this Letter, the nanostructure and electrical properties of post-implanted annealed Cu films by 30 keV nitrogen ions with different doses have been discussed. For this purpose, two series of samples were prepared with deposition of 620 nm- and 390 nm-thick Cu films on Si substrates. The post-implantation annealing for both series of samples was performed at 200°C. The GIXRD patterns confirmed that nitrogen ion implantation at all the applied doses could produce a copper azide phase which was intensified by increasing the ion implantation dose. They showed formation and crystallisation of the $Cu_3N$ phase at the dose of $2.3 \times 10^{18}$ ions/cm$^2$ and annealing time of 180 min at 200°C. According to the AFM results, after post-implantation annealing, the overall trend was a decrease in grain size and the roughness of the copper films. The sheet resistance of the samples in both series increased with increase of the nitrogen ion dose in comparison to that of untreated Cu film because of nitrogen incorporation and the development of $Cu_3N$ as well as the copper azides phase. The sheet resistance variations showed that a higher resistivity can be obtained at higher ion doses and higher annealing time because of the formation of more $Cu_3N$ phases with a semiconductor characteristic. Based on the obtained results, it can be concluded that direct nitrogen ion implantation followed by post-implantation annealing could be utilised to transform a given copper film to a nitride film by the adoption and implementation of proper ion implantation conditions (energy and dose) as well as suitable annealing parameters (temperature, atmosphere and duration).

**5. Acknowledgments:** The authors thank M. Malek for assistance in the ion implantation of the samples. They also thank J. Khamse for assistance in AFM measurements. This work was supported by the Agricultural, Medical and Industrial Research School.

## 6 References

[1] Gonzalez-Arrabal R., Gordillo N., Martin-Gonzalez M.S., Ruiz-Bustos R., Agulló-López F.: 'Thermal stability of copper




doi: 10.1049/mnl.2014.0287

nitride thin films: the role of nitrogen', *J. Appl. Phys.*, 2010, **107**, (10), pp. 103513-1–103513-7
[2] Liu Z.Q., Wang W.J., Wang T.M., Chao S., Zheng S.K.: 'Thermal stability of copper nitride films prepared by RF magnetron sputtering', *Thin Solid Films.*, 1998, **325**, (1–2), pp. 55–95
[3] Wang J., Chen J.T., Yuan X.M., Wu Z.G., Miao B.B., Yan P.X.: 'Copper nitride ($Cu_3N$) thin films deposited by RF magnetron sputtering', *J. Cryst. Growth*, 2006, **286**, (2), pp. 407–412
[4] Ji A.L., Huang R., Du Y., Li C.R., Wang Y.Q., Cao Z.X.: 'Growth of stoichiometric $Cu_3N$ thin films by reactive magnetron sputtering', *J. Cryst. Growth*, 2006, **295**, (1), pp. 79–83
[5] Nosaka T., Yoshitake M., Okamoto A., Ogawa S., Nakayama Y.: 'Thermal decomposition of copper nitride thin films and dots formation by electron beam writing', *Appl. Surf. Sci.*, 2001, **169–170**, pp. 358–361
[6] Navío C., Alvarez J., Capitan M.J., Camarero J., Miranda R.: 'Thermal stability of Cu and Fe nitrides and their applications for writing locally spin valves', *Appl. Phys. Lett.*, 2009, **94**, (26), pp. 263112-1–263112-3
[7] Ji Z., Zhang Y., Yuan Y., Wang C.: 'Reactive DC magnetron deposition of copper nitride films for write-once optical recording', *Mater. Lett.*, 2006, **60**, (29–30), pp. 3758–3760
[8] Niu J., Gao W., Dong X., Guan L., Xie F.: 'First principles calculations of optical properties of $Cu_3N$ and $Cu_4N$', *Adv. Mater. Res.*, 2011, **150–151**, pp. 1290–1293
[9] Venkata Subba Reddy K., Sivasankar Reddy A., Sreedhara Reddy P., Uthannam S.: 'Copper nitride films deposited by dc reactive magnetron sputtering', *J. Mater. Sci. Mater. Electron.*, 2007, **18**, (10), pp. 1003–1008
[10] Nosaka T., Yoshitake M., Okamoto A., Ogawa S., Nakayama Y.: 'Copper nitride thin films prepared by reactive radio-frequency magnetron sputtering', *Thin Solid Films*, 1999, **348**, (1–2), pp. 8–13
[11] Kim K.J., Kim J.H., Kang J.H.: 'Structural and optical characterization of $Cu_3N$ films prepared by reactive RF magnetron sputtering', *J. Cryst. Growth*, 2001, **222**, (4), pp. 767–772
[12] Du Y., Ji A.L., Ma L.B., Wang Y.Q., Cao Z.X.: 'Electrical conductivity and photoreflectance of nanocrystalline copper nitride thin films deposited at low temperature', *J. Cryst. Growth*, 2005, **280**, (3–4), pp. 490–494
[13] Yuan X.M., Yan P.X., Liu J.Z.: 'Preparation and characterization of copper nitride films at various nitrogen contents by reactive radio-frequency magnetron sputtering', *Mater. Lett.*, 2006, **60**, (15), pp. 1809–1812
[14] Maruyama T., Morishita T.: 'Copper nitride thin films prepared by radio-frequency reactive sputtering', *J. Appl. Phys.*, 1995, **78**, (6), pp. 4104–4107
[15] Pierson J.F.: 'Structure and properties of copper nitride films formed by reactive magnetron sputtering', *Vacuum*, 2002, **66**, (1), pp. 59–64
[16] Bhushan B., Gupta B.K.: 'Handbook of tribology: materials, coatings, and surface treatments' (McGraw-Hill, New York, 1991)
[17] Cristina L.J., Vidal R.A., Ferron J.: 'Surface characterization of nitride structures on Cu (001) formed by implantation of N ions: an AES, XPS and LEIS study', *Surf. Sci.*, 2008, **602**, (21), pp. 3454–3458
[18] Prabhawlkar P.D., Kothari D.S., Nair M.R., Raole P.M.: 'XPS studies at various temperatures of nitrogen implanted copper', *Nucl. Instrum. Methods B*, 1985, **7–8**, (1), pp. 147–150
[19] Liu B.X., Zho X., Li H.-D.: 'Thermodynamics and growth kinetical consideration of metal-nitride formation by nitrogen implantation', *Phys. Status Solid. A*, 1989, **113**, (1), pp. 11–22
[20] Herrmann W.A. 'Copper and its compounds', in Herrmann W.A., Brauer G. (Eds): 'Synthetic methods of organometallic and inorganic chemistry, Vol. 5: Copper, silver, gold, zinc, cadmium and mercury' (Thieme Medical Publishers, Georg Thieme Verlag, Stuttgart, 1996)
[21] Patnaik P.: 'A comprehensive guide to the hazardous properties of chemical substances' (John Wiley & Sons, Inc., Hoboken, NJ, 2007, 3rd edn)
[22] Sari A.H., Salem M.K., Shoorche A.: 'Effect of nitrogen ion implantation in copper', *J. Fusion Energy*, 2011, **30**, (4), pp. 323–327
[23] Skelly J.F., Bertrams T., Munz A.W., Murphy M.J., Hodgson A.: 'Nitrogen induced restructuring of Cu(111) and explosive desorption of $N_2$', *Surf. Sci.*, 1998, **415**, (1–2), pp. 48–61
[24] Park J.Y., Kwon T.H., Koh S.W., Kang Y.C.: 'Annealing temperature dependence on the physicochemical properties of copper oxide thin films', *Bull. Korean Chem. Soc.*, 2011, **32**, (4), pp. 1331–1335
[25] Pletea M., Brückner W., Wendrock H., Kaltofen R.: 'Stress evolution during and after sputter deposition of Cu thin films onto Si(100) substrates under various sputtering pressures', *J. Appl. Phys.*, 2005, **97**, (5), pp. 054908-1–054908-7
[26] Mech K., Kowalik R., Zabinski P.: 'Cu thin films deposited by DC magnetron sputtering for contact surfaces on electronic components', *Arch. Metall. Mater.*, 2011, **56**, (4), pp. 903–908
[27] Choi H.M., Choi S.K., Anderson O., Bange K.: 'Influence of film density on residual stress and resistivity for Cu thin films deposited by bias sputtering', *Thin Solid Films*, 2000, **358**, (1–2), pp. 202–205
[28] Chawla J.S., Gstrein F., O'Brien K.P., Clarke J.S., Gall D.: 'Electron scattering at surfaces and grain boundaries in Cu thin films and wires', *Phys. Rev. B*, 2011, **84**, (23), pp. 235423-1–235423-10
[29] Lim J.W., Mimura k., Isshiki M.: 'Thickness dependence of resistivity for Cu films deposited by ion beam deposition', *Appl. Surf. Sci.*, 2003, **217**, (1–4), pp. 95–99